Preprints.org

Communication

Not peer-reviewed version

Pre-launch Multi-Energy Radiance Calibration of the Oms-N

Jinghua Mao , Yongmei Wang * , Entao Shi , Xiuqing HU , Qian Wang , Jinduo Wang

Posted Date: 30 October 2023

doi: 10.20944/preprints202310.1898.v1

Keywords: radiance; integrating sphere; calibration

Preprints.org is a free multidiscipline platform providing preprint service that is dedicated to making early versions of research outputs permanently available and citable. Preprints posted at Preprints.org appear in Web of Science, Crossref, Google Scholar, Scilit, Europe PMC.

Copyright: This is an open access article distributed under the Creative Commons Attribution License which permits unrestricted use, distribution, and reproduction in any medium, provided the original work is properly cited.

Preprints (www.preprints.org) | NOT PEER-REVIEWED | Posted: 30 October 2023 doi:10.20944/preprints202310.1898.v1

Disclaimer/Publisher's Note: The statements, opinions, and data contained in all publications are solely those of the individual author(s) and contributor(s) and not of MDPI and/or the editor(s). MDPI and/or the editor(s) disclaim responsibility for any injury to people or property resulting from any ideas, methods, instructions, or products referred to in the content.

Communication

Pre-Launch Multi-Energy Radiance Calibration of the OMS-N

Jinghua Mao [1,3,4], Yongmei Wang [1,2,3,4,*], Entao Shi [1,3,4] ,Xiuqing Hu [5] and Qian Wang [5] and Jinduo Wang [6]

[1] Laboratory of Space Environment Exploration, National Space Science Center, Beijing 100190, China; e-maojinghua@nssc.ac.cn (J.M.); wym@nssc.ac.cn (Y.W.); set@nssc.ac.cn (E.S.); huxq@cma.gov.cn(Q.H.); qwang@cma.cn(Q.W.);jinduo_cas@163.com (J.W.)
[2] School of Astronomy and Space Science, University of Chinese Academy of Sciences, Beijing 100049, China
[3] Beijing Key Laboratory of Space Environment Exploration, Beijing 100190, China
[4] Key Laboratory of Environmental Space Situation Awareness Technology, Beijing 100190, China
[5] National Satellite Meteorological Centre,Beijing 100081,China
[6] National Key Laboratory of Scattering and Radiation, Beijing 100854, China
* Correspondence: wym@nssc.ac.cn

Abstract: This paper presents the prelaunch radiometric calibration of the Ozone Monitor Suite - Nadir (OMS-N) instrument, a vital payload on the FY-3F satellite. FY-3F achieved a successful launch on August 3, 2023. The radiance calibration of the OMS-N instrument was achieved using an integrating sphere, with known exit radiance ascertained through a transferring radiometer. The calibration model incorporates six energy levels. The Solar Simulator Standard System was employed to validate the calibration results, selecting specific rows to represent varying spatial dimensions. Considering the influence of xenon lamp characteristic peaks and transmission errors during the calibration process, the average deviation remained within 2.3% for the UVIS channel, 3% for the UV1 channel, and 2.2% for the UV2 channel. Furthermore, this study analyzed the uncertainty of the radiometric calibration. The results indicated an absolute uncertainty of 2.32% for both UV1 and UV2 channels, while the VIS channel exhibited an uncertainty of 1.67%. The relative uncertainty was 1.84% for both UV1 and UV2 channels, with the VIS channel exhibiting an uncertainty of 1.45%. The obtained calibration coefficients are accurate and reliable and can be used for the inversion of product parameters, which is of great significance to the quantitative application of satellite data and the advancement of scientific research on quantitative remote sensing.

Keywords: radiance; integrating sphere; calibration

1. Introduction

In recent years, China's space optical remote sensing detection has witnessed rapid development and growth. After years of continuous progress and accumulation, the functionality of China's on-board space probes has matured significantly. This evolution is attributed to the critical role of optical radiation as the fundamental carrier of optical remote sensing information. Consequently, the key application of remote sensing instruments is to achieve the inversion of atmospheric trace component gases through the analysis of atmospheric backscattered spectral radiation, establishing corresponding relationship models in the process. The achievement of high-precision trace gas detection hinges not solely on the performance of the instrument itself but also on the quality of its detection data. In other words, it depends on the extent to which the original data products enable the inversion of target gas content. Within the quantitative inversion of payload detection data, ground radiance calibration [1,2] stands as an irreplaceable and pivotal technology. To ensure the practical value of the quantitative detection results, the radiance calibration accuracy of satellite-based spaceborne optical remote sensing detection instruments has escalated significantly. The primary objective of radiance calibration for on-board high-resolution imaging spectrometers is to calibrate the Digit Number (DN) output of the payload's CCD with the incident DN of the CCD. One

© 2023 by the author(s). Distributed under a Creative Commons CC BY license.

Preprints (www.preprints.org) | NOT PEER-REVIEWED | Posted: 30 October 2023 doi:10.20944/preprints202310.1898.v1

such instrument, the Ozone Monitor Suite - Nadir (OMS-N), is a prominent component of the FY-3(06) satellite payload. The FY-3F satellite comprises 10 remote sensing instruments that offer advanced quantitative remote sensing capabilities, which can effectively improve the accuracy of detection. Based on global imaging and vertical atmospheric detection techniques, FY-3F enables Earth surface imaging, revealing global ozone distribution and monitoring global snow and ice cover, sea surface temperature, natural disasters and ecological environment. It also provides remote sensing information required for short-term climate prediction and climate change prediction, improving the ability to respond to emergencies and upgrading the overall efficacy of meteorological disaster prevention and mitigation. FY-3F will be grouped with other FY-3 satellites in orbit for all-weather meteorological monitoring, improving the accuracy and timeliness of weather forecasting. The OMS-N in FY-3 is expected to provide daily global information and dynamic monitoring of critical atmospheric trace gases that influence air quality and climate change. These gases include total ozone (O_3) and profiles at Nadir, sulfur dioxide (SO_2), nitrogen dioxide (NO_2), BrO, CHOLC, aerosols, and clouds, among others.

OMS-N is a spectrometer designed to measure atmospheric backscattered radiance and solar irradiance within the ultraviolet and visible range, spanning from 250 nm to 495 nm, with a spectral resolution ranging between 0.5 to 1.0 nm. It employs a wide-angle telescope to achieve global coverage on a daily basis.

Ground-based calibrations serve two primary purposes: establishing radiometric sensitivity [3–5] and providing measurement uncertainty data for the payload. On-orbit calibrations [6,7] are subsequently performed to continuously monitor the degradation of payload sensitivity. Regardless of the method or equipment employed for calibration, it is crucial to recognize that calibration results may not be absolutely accurate. Therefore, there is an inherent systematic error in radiation calibration that cannot be entirely eliminated. To meet the stringent radiation calibration accuracy requirements of OMS-N, it is imperative to construct an instrument radiometric response model using a multi-energy approach, involving stable and uniform light sources [8,9]. This method plays a pivotal role in correcting the effects of radiometric nonlinearities in OMS-N.

The radiometric calibration of OMS-N is crucial to the quantification of remote sensing products because it enables the conversion of the electronic information received by OMS-N into real and reliable radiometric values. Moreover, acquiring high-precision quantitative data from OMS-N highly depends on the accuracy of ground-based radiometric calibration. For more accurate data for the inversion of global atmospheric ozone content, this study focused on the pre-launch radiometric calibration of the OMS-N instrument, conducted under vacuum conditions. The factors affecting the OMS-N radiative transfer link were comprehensively analyzed, and multi-energy-level radiometric calibration methods were investigated through laboratory validation tests. Subsequently, a radiance response model and coefficients for in-flight conditions were derived. Additionally, we established a straightforward validation approach to test and refine the calibration results. This study makes scientific and application-oriented contributions, achieving remote sensing data of replacement products that conform to the expected quality standards.

2. Instrument Description

The OMS-N is a wide field-of-view (FOV) imaging spectrograph, employing two CCDs as detectors to facilitate simultaneous spectral and spatial imaging. One dimension on the CCD corresponds to the expansive FOV across the track in the flight direction, while the other dimension registers the spectrum. Table 1 provides an overview of critical OMS-N specifications.

OMS-N features three spectral channels with two CCDs, comprising the UV1 channel (wavelength range: 250-300 nm), the UV2 channel (wavelength range: 300-320 nm), and the visible channel (wavelength range: 310-495 nm). The primary objective of radiance calibration is to establish a mathematical relationship between the DN output of the OMS-N and the radiance of the incident light. However, due to the presence of ambient background radiation and the spectral, temporal, and polarization variability of radiance, achieving high-precision radiance calibration is a notably challenging and complex task.

Preprints (www.preprints.org) | NOT PEER-REVIEWED | Posted: 30 October 2023 doi:10.20944/preprints202310.1898.v1

Table 1. Specifications of OMS-N.

Index	Characteristics		
Scientific Objectives	O_3, SO_2, NO_2, BrO, O_3 profile, Aerosol, Cloud, etc		
Channel	UV1	UV2	UVIS
Spectral range/nm	250-300 nm	300-320 nm	310-495 nm
Spectral resolution/nm	~1	0.5	~0.6
Field of View	112°		
Spatial resolution	28 km × 21 km (at nadir)	7 km × 7 km (at nadir)	7 km × 7 km (at nadir)
SNR	>50	＞200	＞200@ UV >1000 @ VIS
Wavelength calibration accuracy	0.05 nm	0.05 nm	0.05 nm
Relative radiometric calibration accuracy	2%	2%	2%
Absolute radiometric calibration accuracy	3%	3%	3%

Figure 1 illustrates the block diagram depicting the operational principle of OMS-N. Atmospheric backscattered radiation enters the instrument through the primary mirror of the wide-angle telescope system, where it is reflected and subsequently deflected by the depolarizer. The second mirror within the super wide-angle telescope system converges the light onto the incident slit of the spectrometer. A dichroic mirror divides the light into two components: one directed to the UV1-UV2 channel through a plane grating, passing through the imaging objective lens, and eventually forming an image on the FPA of the CCD detector. The other component is routed to the UV-Vis channel, similarly coupled by a plane grating and imaging objective lens, before reaching the CCD detector.

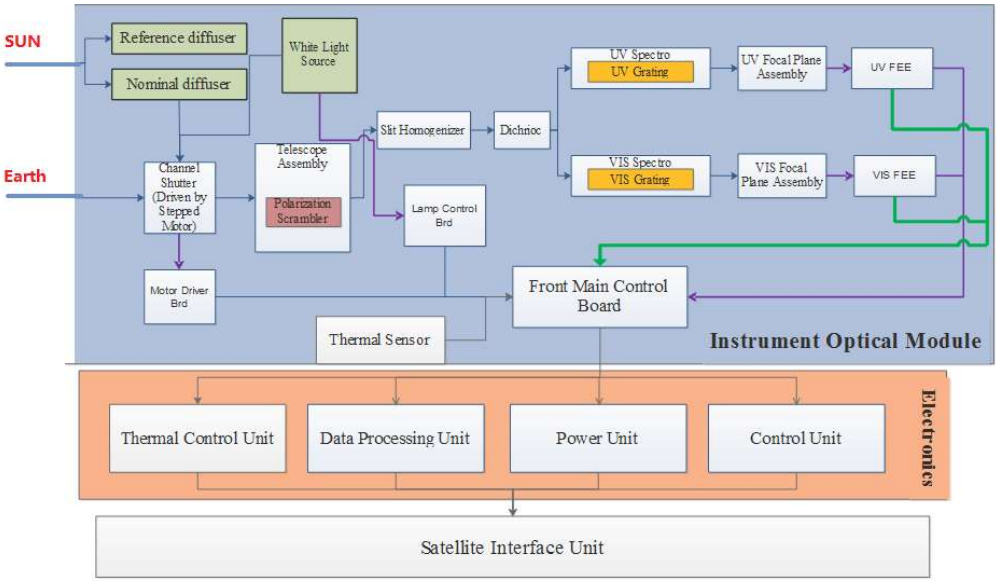

Figure 1. Functional Schematic of the OMS-N.

To ensure long-term stability and a lifespan exceeding 8 years, on-orbit calibration plays a pivotal role. Two diffusers are utilized for measuring solar irradiance, and wavelength shift monitoring is achieved by exploiting solar Fraunhofer lines during solar calibration. Additionally, a white-light source serves as an inter-calibration reference for detector performance.

Temperature control for the optical bench and detector module is accomplished through a passive radiator plate. The operational temperature of the optical bench is maintained at 20 ± 2 K, while the detector operates at a lower temperature of 243 K.

Preprints (www.preprints.org) | NOT PEER-REVIEWED | Posted: 30 October 2023 doi:10.20944/preprints202310.1898.v1

3. Radiance calibration

3.1. Principle of radiance calibration

Radiance calibration for spaceborne optical imaging spectrometers typically employs one of two methods: [6,7] the first involves a standard diffuser coupled with a 1000W NIST lamp [10], while the second method employs an integrating sphere [11–13]. In the diffuser method [11,14,15], a standard lamp with a known radiance illuminates a standard diffuse reflector, creating a large-area light source of known radiance that then irradiates the target under measurement. The alternative approach utilizes a large-aperture integrating sphere for radiance calibration [16,17]. Due to its uniform exit light distribution and substantial aperture, this method ensures better measurement accuracy of spatial response characteristics. After calibration by a Metrological Institute, the radiance value at the integrating sphere's exit surface can be directly employed for ground-based radiance calibration. The OMS-N is a wide FOV imaging spectrometer with a 112° FOV. Regardless of the chosen radiance calibration method, a single calibration cannot cover the entire field of view. Consequently, the radiance calibration process necessitates rotating the instrument through a rotary table in the direction of the Earth port, conducting multiple measurements to complete radiance response calibration.

For the calibration of OMS-N, an integrating sphere is used as a standard light source. The radiance emitted from the integrating sphere is adjustable, and the radiance at each energy level is calibrated using a radiometer that has been directly calibrated by a black body. Different light sources are selected for radiometric calibration based on different spectral channels of OMS-N. The integrating sphere system comprises a xenon lamp for calibrating the UV channel and a tungsten lamp for calibrating the visible channel. Xenon lamps yield high output energy at 250-320 nm and characteristic peaks near long-wave 460 nm, which can enhance the accuracy of radiometric calibration at 460 nm, and tungsten halogen lamps are exceedingly low in energy at 250-300 nm but exhibit smooth spectral curves at 310-493 nm. Given the OMS-N's 112° FOV, a single illumination can only cover a 2° portion of the field of view. Consequently, it is necessary to adjust the turntable 57 times during calibration to cover the full OMS-N field of view. To account for the OMS-N's non-linearity, the integrating sphere is controlled to output different spectral radiances at six levels (L(i), i=1,2,3,4,5,6). Radiance calibration is conducted at each energy level, and finally, radiance sensitivity is fitted using Formula 1:

$$L(row,col) = R_1(row,col) \bullet DN^2(row,col) + R_2(row,col) \bullet DN(row,col) + R_3(row,col) \quad (1)$$

where row and col represent the pixel position, $L(\mathrm{row},\mathrm{col})$ represents the radiance of the pixel ($\mu W/cm^{-2}.str.nm$), R_n (n=1,2,3) represents the radiance responsivity of the pixel, and $DN(\mathrm{row},\mathrm{col})$ represents the signal counts after subtracting the dark background.

During calibration, 50 frames of signal and dark images are captured each time, from which the pure signal is obtained using Equation 2:

$$DN(row,col) = \frac{1}{50}\sum_{j=1}^{50} DN_{sphere}(row,col,j) - \frac{1}{50}\sum_{j=1}^{50} DN_{dark}(row,col,j) \quad (2)$$

where row and col represent the pixel position, j represents the number of captures, DN_{sphere} represents the light signal, DN_{dark} represents the dark signal, and $DN(row,col)$ represents the signal counts after subtracting the dark background.

Preprints (www.preprints.org) | NOT PEER-REVIEWED | Posted: 30 October 2023 doi:10.20944/preprints202310.1898.v1

3.2. Calibration setup

An integrating sphere serves as the standard radiance source, and a transfer radiometer is employed to measure the primary radiance source. An NIST lamp and a NIST standard diffuser are used for verification of calibration results. The calibration schematic is depicted in Figure 2.

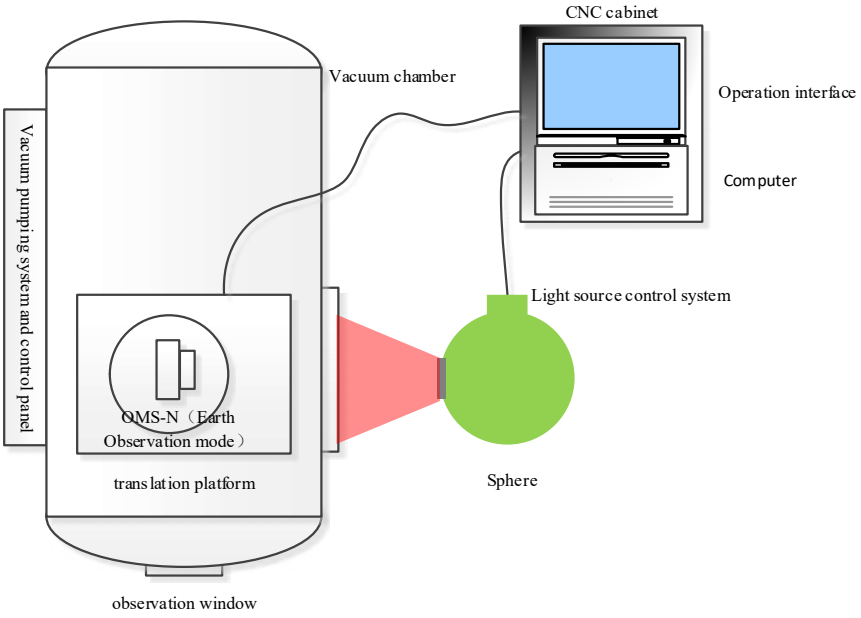

Figure 2. The radiance calibration schematic of OMS-N.

a. Five-dimensional rotating station

The target load is mounted on a five-dimensional rotating platform capable of translation in three directions and rotation along two axes. This platform enables field scanning to calibrate each pixel on the image plane.

b. Integrating Sphere

A 200cm diameter integrating sphere with a 20cm exit port diameter was utilized. Its inner surface was coated with polytetrafluoroethylene. Eight external 1000-W halogen tungsten lamps and two internal 300-W xenon lamps served as light sources within the sphere. A Labsphere interior integrated silicon unit detector (5-mm) was connected to a Labsphere electrostatic meter via a Bayonet Neill–Concelman interface to monitor sphere radiance stability. A 10-level adjustable diaphragm was positioned between each external tungsten lamp source and the sphere entrance. During calibration, the sphere was placed externally to the thermal-vacuum chamber, fully illuminating the instrument entrance slit through a window.

c. Transfer Radiometer

To calibrate the radiometric characterization of the calibration system, the intensity field of the integrating sphere was measured. The radiometer's original calibration certificate was traceable to the National Institute of Metrology (NIM). We calibrated the radiometer using a blackbody, with a spectral radiance scale uncertainty of 2% (k = 2) for the radiometer.

d. Solar Simulator Standard System (SSSS)

Designed primarily to verify OMS-N's radiance calibration results, this system consists of a solar simulator and a diffuser. The simulator employs reflective off-axis optical design and utilizes a 3000W lamp as a source with superior UV intensity. The simulator's spectral radiance scale uncertainties (k = 2) are 2.1%. A Labsphere diffuser is employed for spectral radiance standard transfer from the lamp

Preprints (www.preprints.org) | NOT PEER-REVIEWED | Posted: 30 October 2023 doi:10.20944/preprints202310.1898.v1

to OMS-N and the radiometer via an apparatus. This apparatus, positioned at 700 mm from the diffuser's center, holds the simulator normal to the diffuser's surface. Calibration coefficients were verified by comparing radiance values obtained from the radiometer with those calculated by OMS-N.

4. Results and discussion

4.1. Radiance Calibration

The OMS-N boasts a 112° field of view, with each illumination covering only 2° of this expansive expanse. Consequently, the spatial dimension of the CCD encompasses just five rows at a time. By skillfully adjusting the turntable multiple times, we assemble a comprehensive focal plane signal map from data collected at various angles, as illustrated in Figure 3. The apparent division in Figure 3 (a) arises due to different gain settings on either side of the detector.

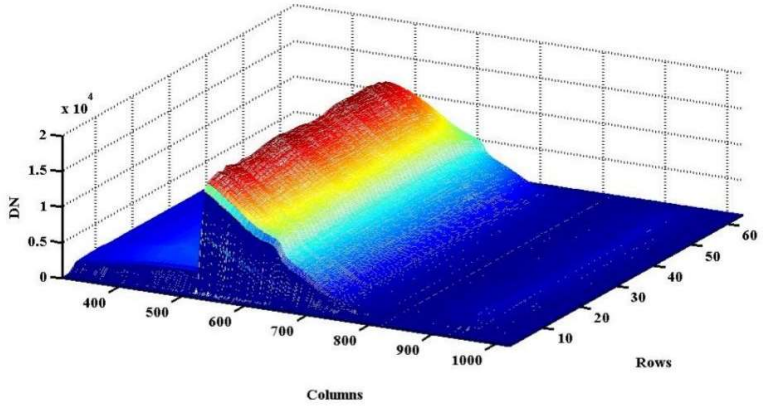

(a) UV1

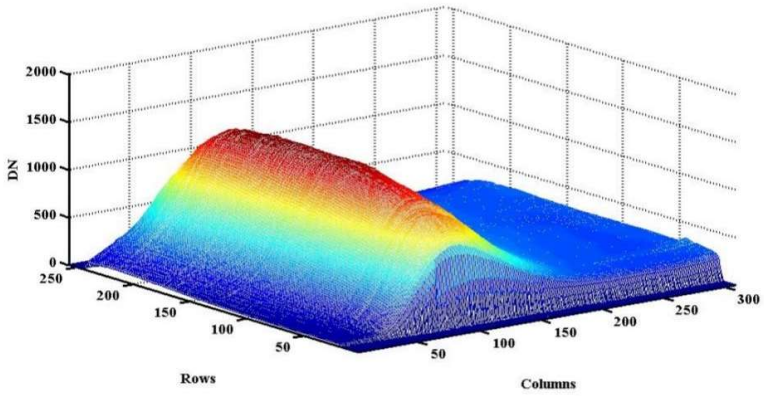

(b) UV2

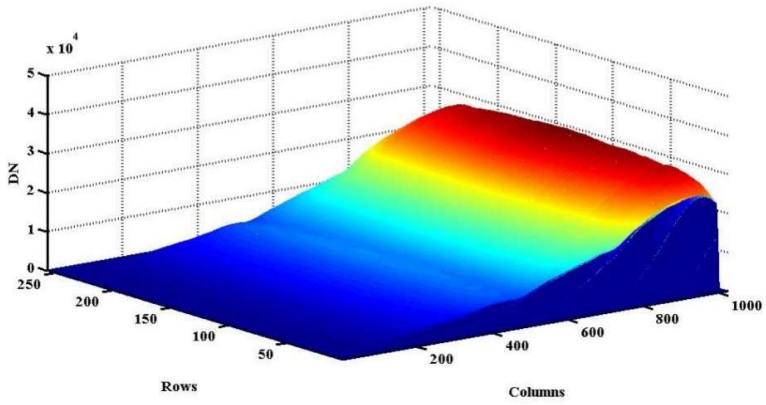

(c) VIS

Preprints (www.preprints.org) | NOT PEER-REVIEWED | Posted: 30 October 2023 doi:10.20944/preprints202310.1898.v1

Figure 3. Signal map of the OMS-N CCD after the splicing of the three channels.

Applying Equations 1 and 2, the signal maps acquired at the six energy levels were fitted to the radiance of the integrating sphere, a value derived through radiometer calibration. The objective was to calculate the fitting coefficients. The distribution of these coefficients is visually represented in Figure 4.

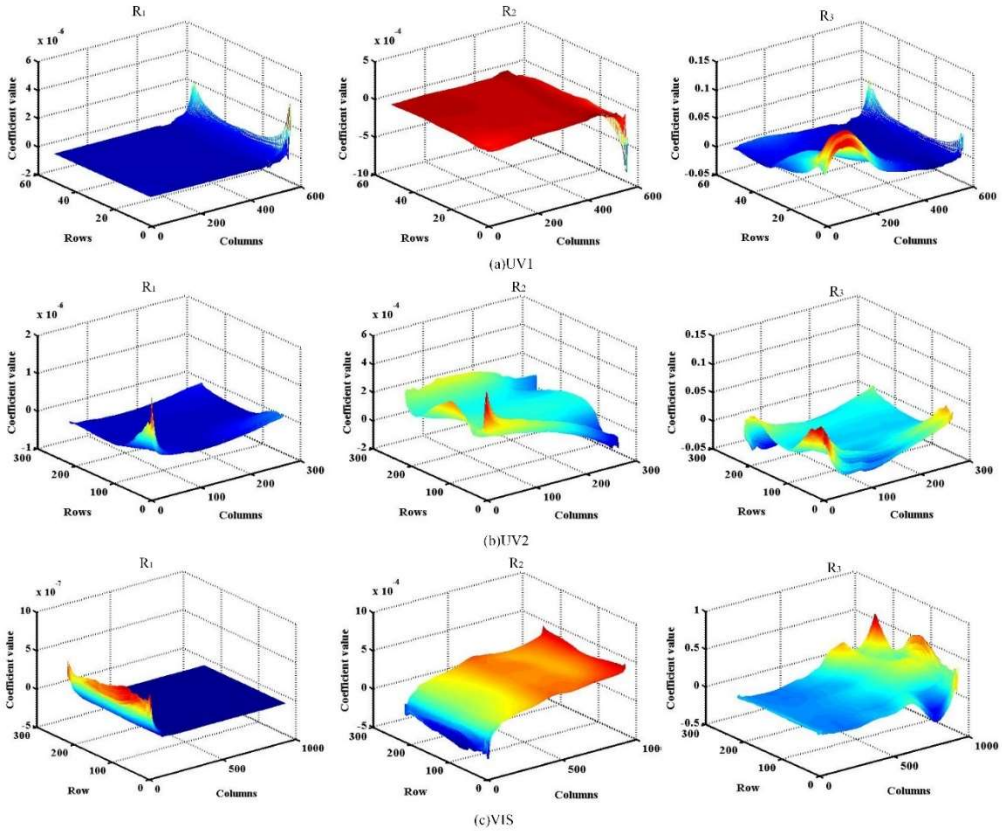

Figure 4. Distribution of fitting coefficients for full pixel radiance calibration.

To validate the multi-energy level fitting coefficients, we employ data obtained from the Solar Simulator Standard System (SSSS). After subtracting the dark background from images captured with the SSSS and substituting the calibration coefficients, we calculate radiance values. We then compare these calculated values with standard values to ascertain the accuracy of the fitting results. Figure 5 displays the radiance values of the OMS-N in the central field of view alongside the standard radiance values from the transfer radiometer. The discrepancy between these two sets of values is elucidated in Figure 6. For validation purposes, we select various rows indicating different spatial dimensions. In the case of the UVIS channel, distinct colors represent different spatial rows—specifically, rows 15, 30, 45, 60, 75, 90, 105, 120, 135, 150, 165...243. Rows 5, 8, 11, 14, 17, 20, 23, 26, 29, 32, 35...61 are selected for UV1, considering the wavelength of 270 nm to 300 nm. For the UV2 channel, rows 18, 33, 48, 63, 78, 93, 108, 123, 138, 153, 168...239 are selected. Radiance comparison is not performed in the 250 nm to 270 nm range to prevent lower signal-to-noise ratios and increased errors. Considering xenon lamp characteristic peaks, the average deviation remains within 2.8% for VIS, 3% for UV1, and 2.2% for UV2. This deviation can be attributed to transmission errors encountered during the calibration process. As Figure 6(a) demonstrates, signal fluctuations are more pronounced in the shortwave UV, stemming from the lower signal-to-noise ratio in the UV band between 250-270 nm. Consequently, subsequent results in this text exclusively pertain to the 270-493 nm range.

Preprints (www.preprints.org) | NOT PEER-REVIEWED | Posted: 30 October 2023 doi:10.20944/preprints202310.1898.v1

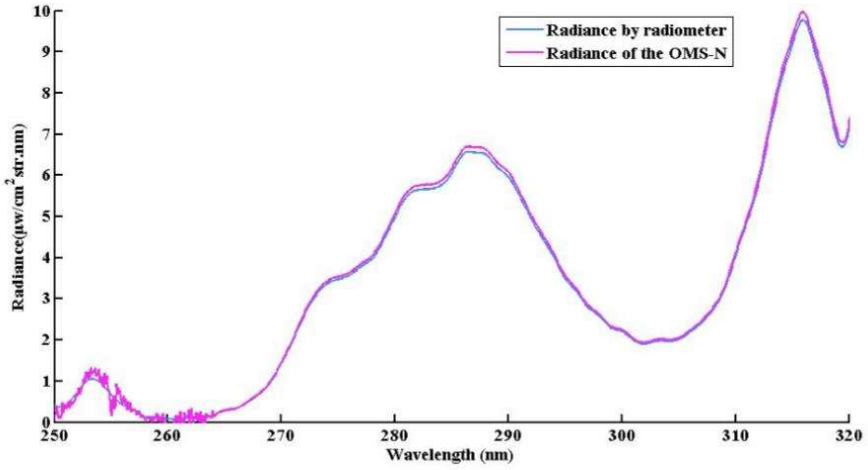

(a) UV

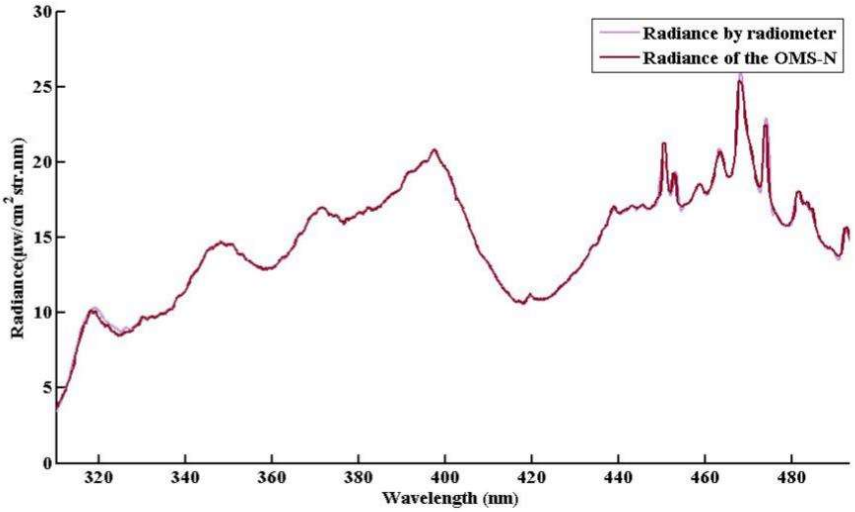

(b) VIS

Figure 5. Radiance distribution in the infra-stellar field of view, obtained through OMS-N calculations and radiometry.

Preprints (www.preprints.org) | NOT PEER-REVIEWED | Posted: 30 October 2023 doi:10.20944/preprints202310.1898.v1

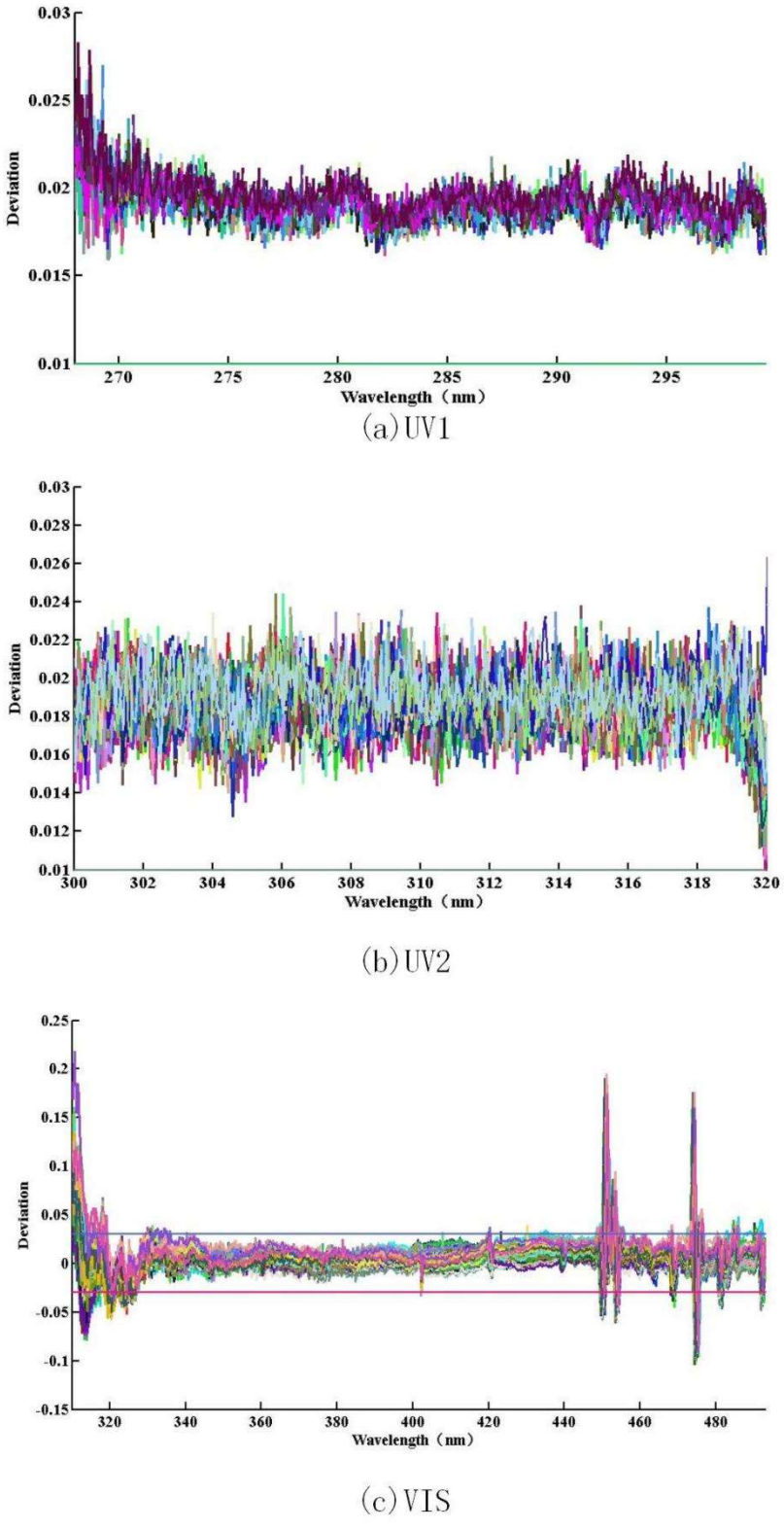

Figure 6. Comparative distribution of multi-field calibration errors.

4.2. Uncertainty of radiance calibration

The absolute accuracy of the OMS-N encompasses factors such as black body traceability of transfer radiometers at the National Institute of Metrology (NIM), OMS-N instability, and source non-uniformity. Table 2 summarizes these results.

Preprints (www.preprints.org) | NOT PEER-REVIEWED | Posted: 30 October 2023 doi:10.20944/preprints202310.1898.v1

Table 2. Absolute accuracy of OMS-N.

Channel	Transfer radiometer uncertainty	Source non-uniformity	OMS-N instability	Total uncertainty
UV	2.1%	0.9%	0.42%	2.32%
VIS	1.33%	0.9%	0.47%	1.67%

Relative radiometric accuracy serves as an indicator of instrument response homogeneity. To assess the relative accuracy of the calibration, we utilized the calibration system to record the output at a given radiance input. For instance, for a specific spectral column, the relative uncertainty for all spatial data under uniform illumination can be expressed by Formula 3:

$$\delta_{\lambda} = \frac{\sqrt{\sum_{i=1}^{n}\left(L_i - \overline{L}\right)^2}}{\overline{L}} \times 100\% \tag{3}$$

L_i represents the DN value of the ith row, $\overline{L}$ represents the average value of all the rows, and δ_λ represents the spatial column response non-uniformity. The variation of relative accuracy with wavelength is depicted in Figure 7. The average relative uncertainties for UV and VIS are 1.84% and 1.45%, respectively.

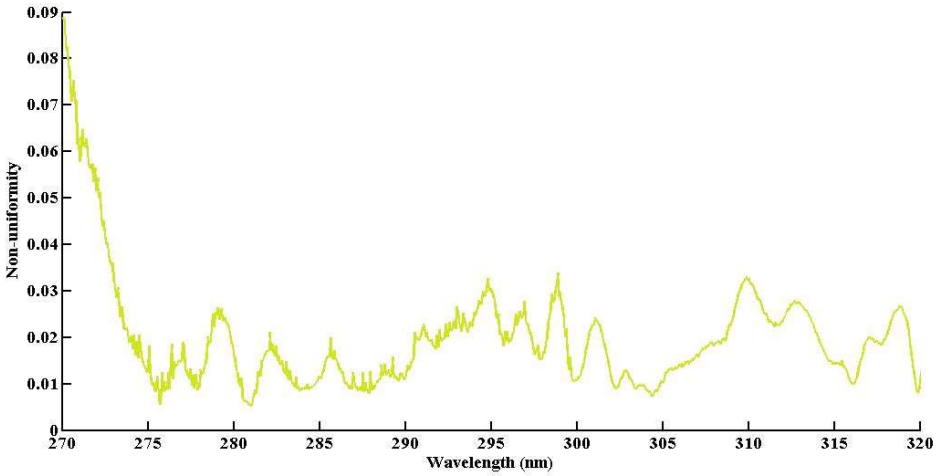

(a) UV1 and UV2

Preprints (www.preprints.org) | NOT PEER-REVIEWED | Posted: 30 October 2023 doi:10.20944/preprints202310.1898.v1

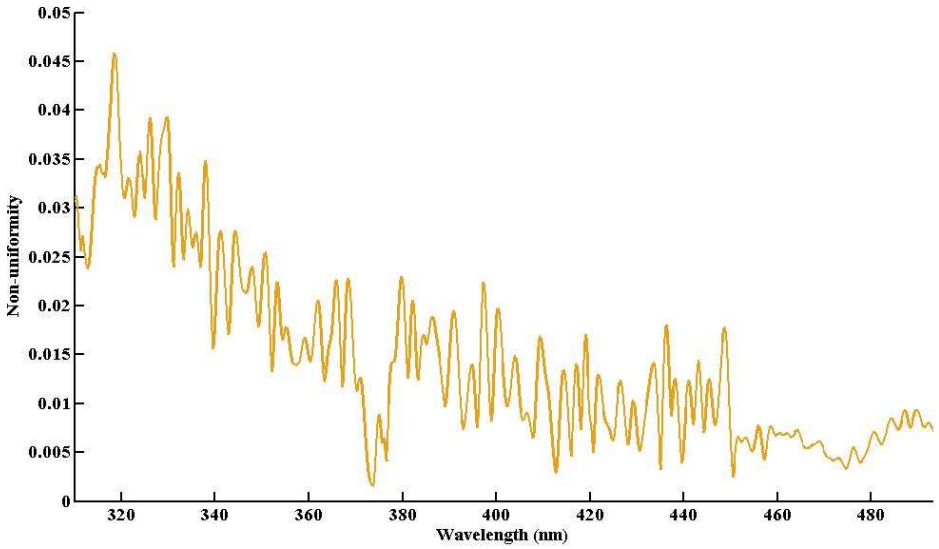

(b) VIS

Figure 7. Variation of relative accuracy with wavelength.

5. Conclusions

The Ozone Monitor Suite - Nadir (OMS-N) is a crucial payload aboard the FY-3F satellite, primarily tasked with dynamically monitoring the total global ozone budget and the column density of various trace gases. It accomplishes this by detecting solar backscatter radiation within the ultraviolet and visible wavelength ranges. OMS-N operates through three spectral channels utilizing two charge-coupled devices (CCD): the UV1 channel spans wavelengths from 250 to 300 nm, the UV2 channel ranges from 300 to 320 nm, and the visible channel covers 310 to 495 nm. Additionally, OMS-N boasts an impressive 112° field of view. As highlighted earlier, the accuracy and stability of radiometric calibration play pivotal roles in achieving high-precision retrievals of global atmospheric concentrations. The successful launch of OMS-N on August 3, 2023, marked a significant milestone, and the pre-launch calibration results have been seamlessly integrated into the data preprocessing procedures. This paper has elucidated the pre-launch radiometric calibration method and radiometric model, both constructed through a multi-level approach to derive the necessary calibration coefficients. These calibration results underwent rigorous verification using the Solar Simulator Standard System. An in-depth analysis of the radiometric calibration's uncertainty revealed that the absolute uncertainty for the UV calibration stood at 2.32%, while for VIS, it was 1.67%. Furthermore, the relative uncertainty for the UV was determined to be 1.84%, with the VIS exhibiting an uncertainty of 1.45%. The OMS-N pre-launch radiometric calibration is the working basis for evaluating the instrument's post-launch radiometric performance. The relevant performance indicators will be analyzed and assessed through post-launch performance tests to obtain high-quality hyperspectral data and excellent radiometric performance, thus contributing to the advancement of quantitative meteorological applications.

Author Contributions: Writing—original draft preparation J.M.; on-ground calibration, J. M., Y. W.; OMS-N instrument designing, E.S.; calibration data-processing program, J.M. and J.W.; writing—review and editing, Y.W., J.M. All authors have read and agreed to the published version of the manu-script.

Funding: This work was supported by the New Generation of Atmospheric Composition Detection Technology [E266000740] and the Youth Innovation Promotion Association,Chinese Academy of Sciences [E2217A06].

Data Availability Statement: The data presented in this study are available on request from the author.

Acknowledgments: The authors wish to thank the FY-3F Project team, Zongyao Ou and Guojun Du from the Beijing Institute of Space Mechanics & Electricity (BSME), Professor Xiuqing Hu and Qian Wang from the National Satellite Meteorological Center.

Preprints (www.preprints.org) | NOT PEER-REVIEWED | Posted: 30 October 2023 doi:10.20944/preprints202310.1898.v1

Conflicts of Interest: The authors declare no conflict of interest.

References

1. Veefkind, J.P.; Aben, I.; Mcmullan, K.; Forster, H.; de Vries, J.; Otter, G.; Claas, J.; Eskes, H.J.; de Haan, J.F.; Kleipool, Q.; et al. TROPOMI on the ESA Sentinel-5 Precursor: A GMES mission for global observations of the atmospheric composition for climate, air quality and ozone layer applications. *Remote Sens. Environ* **2012**, *120*, 70–83.
2. Levelt, P.F.; van den Oord, G.H.J.; Dobber, M.; Eskes, H.; van Weele, M.; Veefkind, P.; van Oss, R.; Aben, I.; Jongma, R.T.; Landgraf, J.; et al. TROPOMI and TROPI: UV/VIS/NIR/SWIR instruments. *Proc. SPIE - Int. Soc. Opt. Eng.* **2006**, *6296*, 385–393.
3. Wang, S.R.; Xing, J.; Li, F.T. Spectral radiance responsivity calibration of ultraviolet remote sensing spectroradiometer in space using integrating sphere. *Opt. Precis. Eng.* **2006**, *14*, 185–190.
4. Xu, Q.; Zheng, X.; Li, Z.; Zhang, W.; Wang, X.; Li, J.; Li, X. Absolute spectral radiance responsivity calibration of sun photometers. *Rev Sci Instrum.* **2010**, *81*, 033103.
5. Lihua C, Ning L, Ciyin Y, Lihong, G., Guoliang, S. Radiance calibration for 3-5 μm infrared detector. *Infrared Laser Eng.* **2012**, *Infrared Laser Eng.* 858-864.
6. de Vries, J.; van den Oord, G.H.J.; Hilsenrath, E.; te Plate, M.; Levelt, P.; Dirksen, R. Ozone Monitoring Instrument (OMI). In *Proc. SPIE. Conf. Imaging Spectrometry VII*; Descour, M.R., Chen, S.S., Eds.; Proc Spie: San Diego, CA, 2001; 1-3, pp. 315–325.
7. Kleipool, Q.; Ludewig, A.; Babic, L.; Bartstra, B.; Braak, R.; Dierssen, W.; Dewitte, P.G.; Kenter, P.; LandzaatM R.; Leloux J.; et al. Pre-launch calibration results of the TROPOMI payload on-board the Sentinel 5 Precursor satellite. *Atmos. Meas. Tech.* **2018**, *11*, 6439–6479.
8. Rosenberg, S.; Maxwell, S.; Johnson, B.C.; Chapsky, L.; Lee, R.A.M.; Pollock, R. Preflight Radiometric Calibration of Orbiting Carbon Observatory 2. *IEEE Trans Geosci Remote Sens* **2017**, *55*, 1994–2006.
9. O'Dell, C.W.; Day, J.O.; Pollock, R.; Bruegge, C.J.; O'Brien, D.M.; Castano, R.; Tkatcheva, I.; Miller, C.E. Preflight Radiometric Calibration of the Orbiting Carbon Observatory. *IEEE Trans Geosci Remote Sens* **2011**, *49*, 2438–2447.
10. Yang, Z.; Zhen, Y.; Yin, Z.; Lin, C.; Bi, Y.; Liu, W., Wang, Q., Wang, L.; Gu, S.; Tian, L. Prelaunch Radiometric Calibration of the TanSat Atmospheric Carbon Dioxide Grating Spectrometer. *IEEE Trans Geosci Remote Sens* **2018**, *56*, 4225–4233.
11. Brown, S.W.; Eppeldauer, G.P.; Lykke, K.R. Facility for spectral irradiance and radiance responsivity calibrations using uniform sources. *Appl Opt.* **2006**, *45*, 8218–8237.
12. Frankenber, C.; Pollock, R.; Lee, R.A.M.; Rosenberg, R.; Blavier, J.F.; Crisp, D.; O'Dell, C.W.; Osterman, G.B.; Roehl, C.; Wennberg, P.O.; et al. The Orbiting Carbon Observatory (OCO-2): spectrometer performance evaluation using pre-launch direct sun measurements. *Atmos Meas Tech.* **2014**, *8*, 301–313.
13. Crisp, D.; Eldering, A.; Gunson, M.R. Preliminary Results from the NASA Orbiting Carbon Observatory-2 (OCO-2). *American Geophysical Union, Fall Meeting* **2014**, abstract id. A52E–01.
14. Klose, J.Z.; Wiese, W.L. Branching ratio technique for vacuum UV radiance calibrations: Extensions and a comprehensive data set. *J Quant Spectrosc Radiat Transf.***1989**, *42*, 337–353.
15. Kuze, A.; Shiomi K, Suto H.; Kataoka, F.; Crisp, D.; Schwandner, F.M.; Bruegge, C.J.; Taylor, T.; Kawakami, S. GOSAT-OCO-2 synergetic CO2 observations over calibration & validation sites and large emission sources. *American Geophysical Union, Fall Meeting* **2015**, abstract id. A41I–0159.
16. Elvidge, C.D.; Baugh, K.E.; Dietz, J.B.; Bland, T.; Sutton, P.C.; Kroehl, H.W. Radiance Calibration of DMSP-OLS Low-Light Imaging Data of Human Settlements. *Remote Sens Environ.* **1999**, *68*, 77–88.
17. Sakuma, F.; Bruegge, C.J.; Rider, D.; Brown, D.; Geier, S.; Kawakami, S.; Kuze, A. OCO/GOSAT Preflight Cross-Calibration Experiment. *IEEE Trans Geosci Remote Sens* **2010**, *48*, 585–599.

Disclaimer/Publisher's Note: The statements, opinions and data contained in all publications are solely those of the individual author(s) and contributor(s) and not of MDPI and/or the editor(s). MDPI and/or the editor(s) disclaim responsibility for any injury to people or property resulting from any ideas, methods, instructions or products referred to in the content.